Materials Science & Engineering A 651 (2016) 83–88

Contents lists available at ScienceDirect

Materials Science & Engineering A

journal homepage: www.elsevier.com/locate/msea

Analysis of partially pulsating fatigue process on carbon steel with microstructural observation

Hiroyuki Shimano [a,*], M. Khairi Faiz [a], Asato Hara [a], Kyoko Yoshizumi [a], Makoto Yoshida [a,b], Susumu Horibe [a]

[a] Department of Modern Mechanical Engineering, Graduate School of Creative Science and Engineering, Waseda University, 3-4-1 Shinjyuku-ku Okubo, Tokyo 169-8555, Japan

[b] Kagami Memorial Research Institute for Materials Science and Technology, Waseda University, 2-8-26, Nishi-Waseda, Shinjyuku-ku, Tokyo 169-0051, Japan

ARTICLE INFO

Article history:
Received 27 July 2015
Received in revised form
19 October 2015
Accepted 26 October 2015
Available online 27 October 2015

Keywords:
Carbon steel
Fatigue
Plastic strain amplitude
Ratcheting strain rate
TEM

ABSTRACT

Pulsating low-cycle fatigue processes, up to the present, have been divided into three states: the transient state, steady state, and accelerating state of ratcheting. In our previous work, we suggested that fatigue behavior of pulsating fatigue process should be classified into five stages in which the plastic strain amplitude and the ratcheting strain rate are plotted on the *X* and *Y* axis, respectively. In this study, at the condition of $R=-0.3$ (partially pulsating fatigue), the change in the plastic strain amplitude and ratcheting strain rate for each cycle to failure was examined on AISI 1025 carbon steel. The dislocation substructure was examined using transmission electron microscopy (TEM) for each stage, except for stage I. It was also demonstrated that the fatigue process can be divided into five stages: stage I corresponds to the un-pinning of dislocations from the Cottrell atmosphere and propagation of the Luders band. Stage II corresponds to the restriction of dislocation movement by dislocation tangles. Stage III corresponds to the formation of dislocation cells. Stage IV corresponds to the promotion of the to-and-fro (back-and-forth) motion of dislocations by a re-arrangement of the dislocations in the cells. Stage V corresponds to the release of dislocation movement by the collapse of dislocation cells.

1. Introduction

Structural materials are often subjected to cyclic loading with non-zero mean stress. In this case, the materials are damaged not only through fatigue damage caused by the plastic strain amplitude but also due to ratcheting damage, i.e., an accumulation of unidirectional inelastic deformation. While structural materials should be generally designed not to cause fatigue fracture, materials have been subjected to unexpected cyclic loading with non-zero mean stress, e.g., in severe earthquakes such as the Great East Japan Earthquake. It is known that ratcheting damage dramatically decreases fatigue life [1–3]. Therefore, many studies have been performed to understand this ratcheting behavior. In previous works on pulsating low-cycle fatigue, ratcheting phenomenon had been divided into three states: the transient state, steady state, and accelerating state. This fatigue process was explained by the cyclic hardening and softening; cyclic softening promotes the accumulation of ratcheting strain and vice versa [4,5]. On the other hand, Kunz et al. [6,7] performed load-controlled asymmetrical cycling for P91 steel. These authors investigated the relationship between the instantaneous plastic strain amplitude and the cyclic creep rate for a constant mean stress, in which the relationship between these two parameters were determined in a log–log graph. Thus, it can be assumed that the relationship between the two damages should be closely interrelated. Nonetheless, the discussions of these studies were limited to only a part of the cycle. The relationship during the entire fatigue process was not discussed.

Meanwhile, in our previous work [8], we proposed a new concept to classify fatigue behavior of pulsating fatigue process. The ratcheting strain rate ($d\varepsilon_r/dN$) is plotted against the plastic strain amplitude ($\Delta\varepsilon_{pl}$) for each cyle to failure, in a log–log graph. As a matter of convenience, hereafter, we define the relationship as ($d\varepsilon_r/dN$ vs. $\Delta\varepsilon_{pl}$) curve. For reference, in [8] we defined the relationship as SH curve, named after Dr. Susumu Horibe who proposed this relationship. The ($d\varepsilon_r/dN$ vs. $\Delta\varepsilon_{pl}$) curve indicated that the fatigue process of AISI 1025 carbon steel should be divided into five stages, which correspond to the transient and accelerating state of previous works. By using this newly proposed curve, a more detailed fatigue process can be observed and explained for a pulsating fatigue process. However, the study discussed only fully repeated loading (stress ratio $R=0$), where the plastic strain

* Corresponding author. Fax: +81 3 5286 3329.
E-mail address: tales-of-destiny@akane.waseda.jp (H. Shimano).

http://dx.doi.org/10.1016/j.msea.2015.10.103
0921-5093/

amplitude is restricted due to the absence of compressive stress. Except for stage II and stage III, the dislocation substructure was not examined. Thus, the grounds for the classification were not necessarily sufficient. In this study, the partially pulsating fatigue process ($R=-0.3$) was examined by analyzing the ($d\varepsilon_r/dN$ vs. $\Delta\varepsilon_{pl}$) curve and dislocation substructure by TEM.

2. Experimental procedures

In this study, AISI 1025 was used as the test specimen. The chemical composition is shown in Table 1. The specimens were cooled in an electrical furnace to room temperature after heating at 850 °C for 45 min (equivalent to the P structure of Hara et al. [8]). The samples contained ferrite and pearlite structures. The specimens were machined into cylindrical, dumbbell-type shapes with a gauge length and diameter of 13 mm and 5.5 mm, respectively.

To determine the mechanical properties, tensile tests were conducted. An Autograph AG-25TB (Shimadzu Corp.) was used. The crosshead speed was 5×10^{-5} m s^{-1}. The mechanical properties obtained are presented in Table 2.

In the fatigue tests, a hydraulic servo-controlled fatigue-strength-testing machine (EHF-EB100kNT-10L, Shimadzu Corp.) was used. Load-controlled cycling with a stress ratio of $R=-0.3$ was conducted at room temperature. A sine-wave signal was used for the load control. All of the specimens were tested at a frequency of 1 Hz. The maximum applied stress (σ_{max}), stress ratio (R) and fatigue life (N_f) for each test are summarized in Table 3. Test nos. 1–4 in Table 3 are cited from Hara et al. [8]. In this study, the plastic strain amplitude ($\Delta\varepsilon_{pl}$) and ratcheting strain rate ($d\varepsilon_r/dN$) are defined as follows [8]:

$$\Delta\epsilon_{pl} = (r_3 - r_2)/2 \quad (1)$$

$$d\epsilon_r/dN = r_2 - r_1 \quad (2)$$

where r_1, r_2 and r_3 are shown in Fig. 1.

The fatigue test specimens were cut into slices measuring 1 mm in thickness along their cross-sections and punched into disks with a diameter of 3 mm. These disks were twin-jet-polished using a solution of 95% ethanol and 5% perchloric acid at 15 V and −40 °C. The foils were examined using a JEM-1011 operated at 100 kV.

3. Results and discussion

3.1. The relationship between cyclic hardening/softening and ratcheting strain rate

The ($d\varepsilon_r/dN$ vs. $\Delta\varepsilon_{pl}$) curve for $\sigma_{max}=391$ MPa at $R=-0.3$ are presented in Fig. 2(a). For $R=0$ at the same σ_{max}, the ($d\varepsilon_r/dN$ vs. $\Delta\varepsilon_{pl}$) curve is shown in Fig. 2(b) which is cited from Hara et al. [8] who is one of the author for this study. The numbers in the figures indicate the number of cycles. An increase of the plastic strain amplitude i.e. a shift to the right direction of the graph means that the material manifests cyclic softening. Meanwhile, an increase of the ratcheting strain rate i.e. a shift to the upward direction of the graph means that an increase of elongation in the tensile direction. The ($d\varepsilon_r/dN$ vs. $\Delta\varepsilon_{pl}$) curve can be divided into five stages based on the folding points in the curve. Similar stages were observed for all of the conditions in Table 3. The five stages are summarized as follows:

Stage I: increase in both the plastic strain amplitude and ratcheting strain rate
Stage II: a slight increase in the plastic strain amplitude with a rapid decrease in the ratcheting strain rate
Stage III: increase in the plastic strain amplitude and decrease in the ratcheting strain rate
Stage IV: increase in the plastic strain amplitude and a constant ratcheting strain rate
Stage V: a rapid increase in both the plastic strain amplitude and ratcheting strain rate

In previous works [4,5], fatigue processes have been divided into three states: a transient state, steady state, and accelerating state of ratcheting, which have corresponded to cyclic hardening/

Table 1
The chemical composition of AISI 1025 (wt %).

C	Si	Mn	P	S	Cu	Ni	Cr
0.25	0.19	0.53	0.011	0.019	0.15	0.04	0.10

Table 2
Mechanical properties of AISI 1025.

Ultimate tensile strength, $\sigma_{U.T.S.}$ (MPa)	Upper yield point, $\sigma_{U.Y.P.}$ (MPa)	Lower yield point, $\sigma_{L.Y.P.}$ (MPa)	Elongation (%)
483.7	443.9	311.6	48.5

Table 3
Stress ratio (R), maximum stress (σ_{max}), and number of cycles to failure (N_f).

Test No.	Stress ratio (R)	Maximum stress, σ_{max} (MPa)	Number of cycles to failure, N_f (cycle)
1[a]	0	464	1.8×10^2
2[a]	0	439	8.0×10^2
3[a]	0	415	4.0×10^3
4[a]	0	391	1.2×10^4
5	0	381	7.1×10^4
6	−0.3	439	2.5×10^2
7	−0.3	415	9.0×10^2
8	−0.3	391	1.9×10^3
9	−0.3	366	6.3×10^3
10	−0.3	342	2.2×10^4
11	−0.3	334	3.3×10^4

[a] These results are cited from Hara et al. [8].

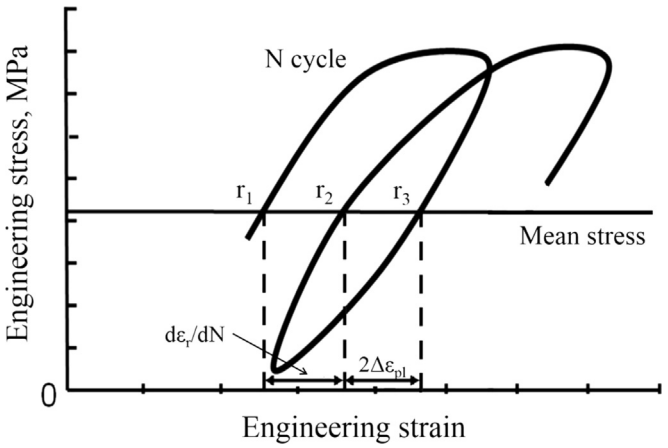

Fig. 1. Engineering stress–engineering strain hysteresis loop at N cycles.